Journal of Materials Chemistry C

A panchromatic electrochromic device composed of Ru(II)/Fe(II)-based heterometallo-supramolecular polymer

Journal:	*Journal of Materials Chemistry C*
Manuscript ID	TC-ART-03-2019-001452.R1
Article Type:	Paper
Date Submitted by the Author:	11-May-2019

Complete List of Authors:	Hsiao, Li-Yin; National Taiwan University, Department of Chemical Engineering Chang, Ting-Hsiang; National Taiwan University, Department of Chemical Engineering; Lu, Hsin-Che; National Taiwan University, Department of Chemical Engineering Wang, Yen-Chun; National Taiwan University, Department of Chemical Engineering Lu, Yen-An; National Taiwan University, Department of Chemical Engineering Ho, Kuo-Chuan; National Taiwan University, Department of Chemical Engineering Higuchi, Masayoshi; National Institute for Materials Science, International Center for Materials Nanoarchitectonics

Journal Name

ARTICLE

A panchromatic electrochromic device composed of Ru(II)/Fe(II)-based heterometallo-supramolecular polymer

Received 00th January 20xx,
Accepted 00th January 20xx

DOI: 10.1039/x0xx00000x

www.rsc.org/

Li-Yin Hsiao,[a, d] Ting-Hsiang Chang,[a] Hsin-Che Lu,[a] Yen-Chun Wang,[a] Yen-An Lu,[a] Kuo-Chuan Ho,[a, b, c]* and Masayoshi Higuchi[d]*

Ru(II)/Fe(II)-based heterometallo-supramolecular polymer (PolyRuFe) has been synthesized and firstly utilized as the working electrode in an electrochromic device (ECD). To obtain a panchromatic characteristic, Prussian blue (PB) is selected as the counter electrode owing to its large absorbance change from 600 to 800 nm, which is complementary to the main absorbance change of PolyRuFe from 400 to 600 nm. When switching between -1.3 and 2.2 V, the proposed ECD utilizing the PMMA gel-typed electrolyte exhibits the transmittance changes (ΔT) of 52.7, 46.9, and 28.0% at 503, 580, and 690 nm, respectively. The fast response times of less than 0.5 s could be observed for both coloring and bleaching processes of the PolyRuFe/PB ECD at 503 and 580 nm. The PolyRuFe/PB ECD also exhibits three-step coloration efficiency and the highest values are 525.1 and 413.6 cm^2/C at 503 and 580 nm, respectively. In addition, the memory effect of PolyRuFe thin film was enhanced by incorporating the multi-walled carbon nanotubes (MWCNT) into PolyRuFe to form PolyRuFe-MWCNT. The relationship between memory effect and mass changes of PolyRuFe and PolyRuFe-MWCNT thin films during redox reaction was monitored by using a quartz crystal microbalance (QCM). The result suggests that the PolyRuFe-MWCNT thin film offers better memory effect than the bare PolyRuFe, due to the adsorption of the perchlorate ions on MWCNT. It is expected that the proposed approach can be applied to other PolyRu electrochromic thin films for improving the long-term stability of the pertinent ECDs.

1. Introduction

The gadget that demonstrates optical change through electrochemical reaction is referred as “electrochromic device (ECD)”. In general, an ECD is composed of both anodically coloring and cathodically coloring materials or one coloring material and one ion storage laye.[1-3] To date, numerous electrochromic (EC) materials have been investigated, such as metal oxides,[4-7] transition metal complexes,[8-10] viologens,[11-14] organic molecules,[15] conductive polymers,[16-19] and metallo-supramolecular polymers (MEPEs).[20-23]

Among all electrochromic materials, metallo-supramolecular polymers draw much attention due to their promising electrochromism as inorganic-organic hybrid materials.[24-26] The polymers show various colors and impressive optical properties owing to metal-to-ligand charge transfer (MLCT) absorption and intervalence charge transfer (IVCT), which are triggered by the electrochemical redox reaction of the metal ions.[27] The concept and definition for the terms of “metallo-supramolecular polymer” and “coordination polymer” are somewhat overlapping. According to the literature, MEPE has been defined as the metal ions either to be an integral part of the polymer chain or are attached to a polymer as pendant side chain.[28] In addition, the interactions between metal ions and ligands have to be strong enough to retain the polymer chain in solution.[29] Recently, terpyridine ligands are most commonly used because of their rich coordination chemistry, thermal stability, and high binding affinity towards a transition metal ions,[30] including Fe(II), Ru(II), Co(II), and other transition metals, which have proved to play a key role in the MEPEs based on d-d* transition or MLCT absorbance.[31-33] Through different ligands and corresponding metal ions combination, new polymers, which exhibit unique electrochromism, can be created.[34] Furthermore, the multi-color characteristic could be observed for the polymers, which utilizing different kinds of ligands or consisting of two metal ion species.[35, 36] In general, the ions in the electrolyte would affect the EC performance of an EC thin film. It has been reported that the anions play a crucial role in the electrochromism of MEPE due to their incorporation during oxidation of a MEPE thin film.[37] Among all of anions, perchlorate ions show the highest current density and the narrowest peak separation potential when switching a

[a] Department of Chemical Engineering, National Taiwan University, No. 1, Sec. 4, Roosevelt Rd., Taipei 10617, Taiwan
[b] Institute of Polymer Science and Engineering, National Taiwan University, No. 1, Sec. 4, Roosevelt Rd., Taipei 10617, Taiwan
[c] Advanced Research Center for Green Materials Science and Technology, National Taiwan University, Taipei 10617, Taiwan
[d] Electronic Functional Macromolecules Group, Research Center for Functional Materials, National Institute for Materials Science (NIMS), Tsukuba 305-0044, Japan
* Email: E-mail: kcho@ntu.edu.tw Fax: +886-2-2362-3040; Tel: +886-2-2366-3020 (K.C. Ho); HIGUCHI.Masayoshi@nims.go.jp Fax: +81-29-860-4721; Tel: +81-29-860-4721 (M. Higuchi)

Ru-MEPE thin film; this suggests that perchlorate ion could be one of the potential anions for the MEPE thin films.

Meanwhile, many researchers aim at developing black-to-transmissive ECD recently for a growing demand of novel displays, which are energy-efficient simultaneously like e-paper or e-book. However, it is a challenging task to achieve high optical change over the entire visible wavelength, and only a few materials have been successfully demonstrated. For examples, Beaujuge et al. reported on the use of the donor–acceptor approach to make a black-to-transmissive polymer thin film.[38] Hsu et al. proposed the Co(II)-based metallo-supramolecular polymer (PolyCo) which showed the black-to-transmissive electrochromism.[39] In addition, some ECDs have been fabricated to possess panchromatic optical change by using multiple EC materials.[40-43] MEPEs draw much attention for high optical contrast, fast response time, and outstanding stability;[32] however, scarcely any of researchers fabricated the ECD which exhibits the panchromatic characteristic based on MEPEs. Although PolyCo exhibits attractive black-to-transmissive characteristic, there are several drawbacks compared with Fe(II) and Ru(II)-based MEPEs; these include a wider potential window and a lack of redox couple that would match with PolyCo.

Compared to other metal complex MEPE, Fe(II)-based and Ru(II)-based MEPE are desirable EC materials for their phenomenal color change upon redox reaction, high coloration efficiency, fast response time and great stability.[44-46] Most importantly, they show the close potential window and specific absorbance around 580 and 503 nm, respectively. Herein, we demonstrate the panchromatic ECD composed of Ru(II)/Fe(II)-based heterometallo-supramolecular polymer (PolyRuFe) and Prussian blue (PB, Iron(III) hexacyanoferrate(II)), for PB provides the strong absorbance from 600 to 800 nm, and PolyRuFe provides the large optical change from 400 to 600 nm. Moreover, anodically coloring PB is selected as the counter electrode in this study because it is a well-known inorganic material with fairly good stability and large optical change.[47, 48] In general, it is operated between two states, one is Prussian blue state (oxidized form) the other is colorless Everitt's salt (ES) (reduced form) and it can be cycled reversibly for more than thousands times in whether aqueous or non-aqueous solvents.[10, 49, 50] Meanwhile, to tackle the leakage problem in a solution-typed electrolyte, the ECD utilize gel-typed electrolyte based on poly-(methyl methacrylate) (PMMA), it leads to safety and well stability of the ECD.[51] It is expected that an ECD exhibits panchromatic absorbance change, fast response time and well cycling stability.

The memory effect is one of the key characteristics for the thin-film type ECD. The memory effect of PolyRuFe was investigated in this study because it was closely related to the long-term stability of the proposed ECD. It is well known that the perchlorate ions from the supporting electrolyte are responsible for charge neutralization with the Fe(II) and Ru(II) ions. It is inferred that the perchlorate ions would be adsorbed or desorbed depending on the oxidation or reduction of the PolyRuFe thin film. Previously, it was reported that the perchlorate ions could be adsorbed effectively on the oxidized CNTs.[52] According to this, the oxidized multi-walled CNTs (MWCNT) were incorporated into the PolyRuFe thin film (PolyRuFe-MWCNT) in the hope to enhance the memory effect in our study. To understand the adsorption and desorption of perchlorate ions in the PolyRuFe thin film during redox reaction, the electrochemical quartz crystal microbalance (EQCM) analysis was applied for the PolyRuFe-MWCNT and the PolyRuFe thin films. The relationship between memory effect and the amount of adsorbed perchlorate ions was confirmed by measuring the mass changes of the PolyRuFe-MWCNT and the PolyRuFe thin films at the open-circuit voltage (OCV).

2. Experimental procedures

2.1. Materials

Indium tin oxide (ITO) glasses were used as the substrates (Solaronix SA, R_{sh}=7 Ω/sq.) and the size of ITO was cut to 3.0 × 4.0 cm^2. The ITO glasses were ultrasonically cleaned by isopropanol for 20 min and then treated with UV ozone for 20 min. The epoxy tapes (3M Company, 60 μm thick) was used to control the active area of 2.0 × 2.0 cm^2 on the ITO glasses surface for the three-electrode system. Sodium ferrocyanide ($Na_4Fe(CN)_6$, >99%), Iron(II) acetate ($Fe(OAc)_2$, >99.99%), 4',4''''-(1,4-Phenylene)bis(2,2':6',2''-terpyridine) (L_0), propyl-ene carbonate (PC, 99.7%), ethylene glycol (EG), methanol (MeOH), acetone (>99%), tetrahydrofuran (THF) were all purchased from Sigma-Aldrich; cis-tetrakis(dimethylsulfoxide)-dichlororuthenium(II) ($RuCl_2(DMSO)_4$, 98%) was purchased from Strem Chemicals, Inc.; sodium perchlorate (anhydrous) was purchased from Wako; methyl methacrylate poymer (PMMA) was purchased from Tokyo Chemical Industry (TCI); iron(III) nitrate ($Fe(NO_3)_3$) was purchased from Nacalai Tesque, Inc. MWCNTs were purchased from Golden Innovation Business Co., Ltd, Taipei, Taiwan, external dia. = 20~40 nm, length = 5~15 mm. All chemicals were used as received without further purification.

2.2. Synthesis of PolyRuFe powder

PolyRuFe powder was synthesized according to the previous literature.[32] First, 108.125 mg (0.2 mmole) L_0 and 48.45 mg (0.1 mmole) $RuCl_2(DMSO)_4$ were mixed and stirred at 150 °C in the 25 ml nitrogen-saturated absolute ethylene glycol (EG) for 24 h. After that, 17.4 mg (0.1 mmole) $Fe(OAc)_2$ dissolved in EG was added to the reaction mixture and stirred at 100 °C in the nitrogen-saturated condition for 24 h. Therefore, the starting molar ratio of Ru:Fe is 1:1. After the reaction, the solution was cooled down to the room temperature and then THF was added in the solution until it turn colorless. The precipitated polymers were collected by filtration and washed two times by THF, and then dried under vacuum overnight to obtain PolyRuFe in >90% yields.

2.3. Synthesis of Prussian blue nanoparticles

For water-dispersible PB nanoparticles, 3.23 g $Fe(NO_3)_3 \cdot 9H_2O$ were mixed with 2.90 g $Na_4Fe(CN)_6 \cdot 10H_2O$ in 45 ml deionized water (DIW).[49, 53] The obtained precipitate was centrifuged at 4,000 rpm for 6 times to remove the residual reactants, and then 0.542 g $Na_4Fe(CN)_6 \cdot 10H_2O$ was added into the mixed solution as surface

modifier and stirred for 3 days. After that, water-dispersible PB nanoparticles were obtained by removing DIW by rotary evaporator.

2.4. Fabrication of the PolyRuFe/PB ECD with gel-typed electrolyte

The PolyRuFe thin film was prepared by spin-coating 100 µl of the polymer solution (4 mg/ml in methanol) at 40 rpm for 5 min. The PB thin film was obtained also by spin-coating 80 µl of the uniformly dispersible aqueous solution (100 mg/ml) at 4,000 rpm for 30 s, and then heated at 90 °C for 30 min. The gel-typed electrolyte was prepared by stirring the $NaClO_4$, PMMA, PC and acetone with the ratio of 3:7:20:70 for 8 h. The PolyRuFe/PB ECD was obtained by sandwiching the gel-typed electrolyte in between the two thin films.

2.5. Preparation of PolyRuFe-MWCNT thin film

First, the nitric acid and MWCNTs were mixed with the ratio of 1 ml:1 mg in a flask at 150 °C for 6 h to prepare the oxidized MWCNTs. The mixture was settling for 24 h, and then neutralised with ammonia solution. The oxidized MWCNTs were washed with deionized water (DIW) several times and dried overnight. After that, 0.5 mg oxidized MWCNTs were dispersed in 1 ml methanol uniformly, and 4 mg of PolyRuFe powder was added in the mixing solvent. The PolyRuFe-MWCNT thin film was prepared by spin-coating 100 µl of the PolyRuFe solution containing MWCNT at 40 rpm for 5 min and finally dried at 50 °C for 30 min.

2.6. Measurements

A potentiostat/galvanostat was used for electrochemical experiments on an ALS/CHI model 612B electrochemical workstation (CH Instruments, Inc.). A conventional three-electrode system was used with the ITO glass as the working electrode, platinum wire as the counter electrode, and a homemade Ag/Ag^+ electrode in ACN with 0.1 M TBAP and 0.01 M $AgNO_3$ as the reference electrode. Spectroelectrochemical measurement was carried out by a spectrophotometer (model DH-2000-BAL, Ocean Optics). CIE (Commission Internationale de l'Eclairage) coordinates of the devices were acquired by using the same spectrophotometer (model DH-2000-BAL, Ocean Optics). An electrochemical quartz crystal microbalance (EQCM, Seiko EG&G, model QCA917) was used for *in situ* study of the mass changes. All electrochemical measurements of the ECD were obtained using the two-electrode configuration. Surface morphologies of the PolyRuFe and PolyRuFe-MWCNT thin films were observed by a field-emission scanning electron microscope (FE-SEM, Nova NanoSEM 230, FEI, Oregon, USA), equipped with an energy dispersive X-ray spectroscopy (EDS, model 7021-H, Horiba, Kyoto, Japan) and field emission transmission electron microscope (FE-TEM, JEOL JEM-2100F, JEOL Ltd., Japan). The PolyRuFe was further characterized by X-ray photoelectron spectroscopy (XPS, Thermo Scientific Theta Probe, East Grinstead, UK).

3. Results and discussion

3.1. Characterization of PolyRuFe

The XPS data of the PolyRuFe for characterizing the Fe(II) and Ru(II) complex are shown in **Figure S1**. In **Figure S1(a)**, the XPS spectra of Fe 2p can be divided into two parts, namely, Fe $2p_{3/2}$ (708 eV) and Fe $2p_{1/2}$ (721.6 eV). The obvious peak at 460.9 eV in **Figure S1(b)** is obtained, which corresponds to Ru $3p_{3/2}$. These results further confirm that the Fe(II) and Ru(II) complex has been assembled successfully. In addition, the EDS spectrum of PolyRuFe is shown in **Figure S2** and the atomic composition is calculated in **Table S1**. It can be seen from the EDS spectrum that the atomic ratio of Fe to Ru is close to 1:1, the same as the starting molar ratio of the two reactants. A cyclic voltammorgram (CV) of PolyRuFe performed in a three-electrode system is shown in **Figure 1(a)**. The first redox couple at 0.77 and 0.70 V could be attributed to the redox between metal ions Fe(II) and Fe(III) and the second redox couple at 0.93 and 0.84 V could be ascribed to the redox between Ru(II) and Ru(III). According to the previous literature of PolyCo,[39] we propose the following electrochromic reaction mechanism for the PolyRuFe thin film, as explained by Eqs. (1) and (2), due to the two-step oxidation of Fe(II) and Ru(II), respectively. When the applied potential bias was more positive than the peak potential at 0.77 V, PolyFe(II)Ru(II) would be oxidized to PolyFe(III)Ru(II), giving a color variation from purple to orange. The color was changed from orange to light green by switching the potential to 0.93 V; this is attributed to the further oxidation of PolyFe(III)Ru(II) to form PolyFe(III)Ru(III).

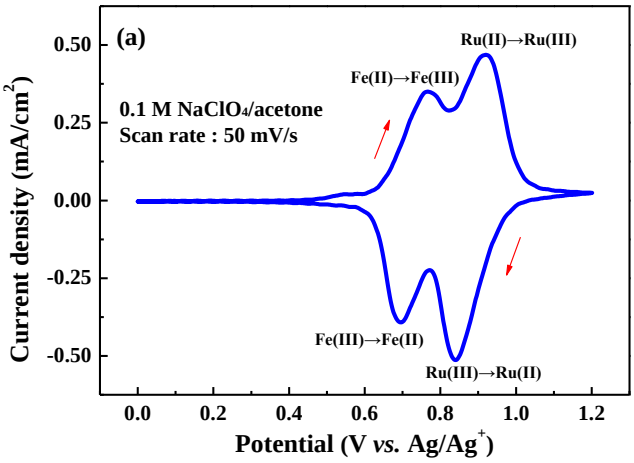

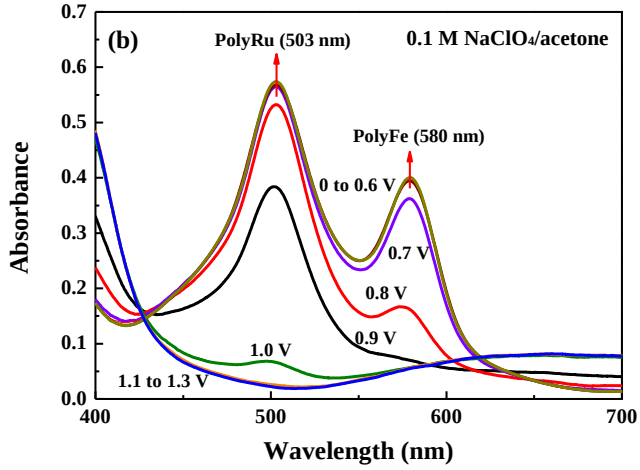

(c)

Figure 1. (a) CV of the PolyRuFe thin film cycled in 0.1 M $NaClO_4$/acetone at 50 mV/s. (b) UV-vis absorbance spectra of the PolyRuFe thin film measured in 0.1 M $NaClO_4$/acetone at different potential biases from 0 to 1.2 V (vs. Ag/Ag^+). (c) Images of PolyRuFe at 1.2 V (bleached state), 0.9 V and 0 V (colored state) in a three-electrode system.

$$[(PolyRu(II)Fe(II)]_n \cdot (4n)ClO_4^- + nClO_4^- \leftrightarrow [(PolyRu(II)Fe(III)]_n \cdot (5n)ClO_4^- + ne^- \quad (1)$$

(purple) (orange)

$$[(PolyRu(II)Fe(III)]_n \cdot (5n)ClO_4^- + nClO_4^- \leftrightarrow [(PolyRu(III)Fe(III)]_n \cdot (6n)ClO_4^- + ne^- \quad (2)$$

(orange) (light green)

where n represents the polymeric number of PolyRuFe.

The absorbance spectra with various applied potential bias are shown in **Figure 1(b)**. Two significantly optical changes occurred with the peaks at 503 nm and 580 nm when the applied potential bias arrived at 1.2 V. PolyRuFe is synthesized with the equimolar ratio of Fe(II) and Ru(II); however, the absorbance of Ru(II) complex portion at 503 nm is much stronger than that of the Fe(II) complex portion at 580 nm. It is attributed to the larger absorption coefficient (ε) value of Ru(II)-based MEPE (PolyRu) than that of Fe(II)-based MEPE (PolyFe). According to the previous literature, the reason is that stronger π-conjugated of ligand (L_0) to the Ru(II) metal ions than to Fe(II) metal ions and a stronger dynamic chelate effect of Ru(II) metal ion to ligand (L_0) compared to that of Fe(II).[32] The images of PolyRuFe at 1.2 V (bleached state), 0.9 V and 0 V (colored state) in three electrode system are shown in **Figure 1(c)**, it shows the multi-color characteristic, the light green, orange and dark purple color could be observed at 1.2, 0.9 and 0 V, respectively.

3.2. UV-vis absorption spectra of water-dispersible PB thin film

A CV of PB performed in a three-electrode system is shown in **Figure S3(a)**. The redox couple could be attributed to the following reaction:

$$Na_4Fe(II)_4[Fe(II)CN_6]_3 \leftrightarrow Fe(III)_4[Fe(II)CN_6]_3 + 4e^- + 4Na^+ \quad (3)$$

(ES, colorless) (PB, blue)

It shows the cycled reversible stability in acetone and the upper applied oxidative potential is controlled at 0.3 V to avoid the appearance of the second redox peak. The absorbance spectra of PB with various applied potential bias are shown in **Figure S3(b)**. When negative potential more than -0.4 V is applied, high transparency was observed. When the applied potential bias reached 0.3 V, a strong absorbance spanned from 600 nm to 1000 nm is noticed and the maximum absorbance peak locates at 690 nm. It is expected that an ECD composed of PolyRuFe and PB would exhibit panchromatic characteristic.

3.3. Characterization of PolyRuFe/PB ECDs

Herein, we fabricated a PolyRuFe/PB ECD. A CV of the ECD is presented in **Figure 2(a)** and three redox peaks could be observed. These two redox couples (a1, c1 and a2, c2) could be described to the redox reaction between PolyRuFe and PB. We propose the mechanism Eq. (4) of the PolyRuFe/PB ECD by combination of Eqs. (1), (2) and (3), as follow:

$$[(PolyRu(II)Fe(II)(ClO_4^-)_4]_n + (n/2)Fe(III)_4[Fe(II)(CN)_6]_3 + 2nNa^+ + 2nClO_4^-$$

(near black)

$$\leftrightarrow [(PolyRu(III)Fe(III)(ClO_4^-)_4]_n + (n/2)Na_4Fe(II)_4[Fe(II)(CN)_6]_3 \quad (4)$$

(light green)

Nevertheless, it is still observed the third redox couple (a3, c3) in the CV measurement. This is attributed to the further reaction between PolyRuFe and PB due to the mismatched charge densities of both PolyRuFe and PB. Owing to the quite small charge density of PolyRuFe, it could not provide sufficient charge to oxidize or reduce PB completely even though PB film is very thin. Thus, the wider potential window is applied such that PB can be fully reacted to achieve a larger transmittance change for the proposed ECD.

In order to investigate electrochromic properties of the PolyRuFe/PB ECD with the gel-typed electrolyte, UV-vis absorbance spectra of the proposed ECD were measured between 2.2 V to -1.3 V, shown in **Figure 2(b)**. The ECD shows panchromatic feature and well absorbance change in the visible region. When the applied negative potential bias reached over -1.3 V, two obvious peaks at 503 nm and 580 nm could be noticed. The large increment at 503 nm and 580 nm are mainly attributed to the redox reaction of Ru(II) and Fe(II) ions, respectively. Similarly, the well optical change could also be perceived from 600 nm to more than 800 nm, and it is mainly described by the redox of PB. Originally, the absorbance of Ru(II) complex portion at 503 nm is much stronger than that of the Fe(II) complex portion at 580 nm, according to the larger absorption coefficient (ε) value of Ru(II)-based MEPE. It could be noticed that the increment of absorbance change at 580nm due to the overlapped absorbance of PB. When the applied potential bias is over 2.2 V, the ECD reach to bleached state; however, the light green is also observed.

The dynamic transmittance curves of the PolyRuFe/PB ECD, which were collected at characteristic absorbance peaks of 503, 580 nm and the absorbance peak of PB at 690 nm, are presented respectively in **Figure 3(a)** (The enlarged view is shown in **Figure S4**). The bleached potential and the coloring potential are 2.3 V and -1.5 V, respectively. The data are also summarized in Table 1. The highest transmittance change (ΔT) of 52.7% at 503 nm could be observed, according to strong π-conjugated of ligand (L_0) to the Ru(II) metal ions. Moreover, the transmittance change (ΔT) of 46.9% and 28.0% could be observed at 580 nm and 503 nm, respectively. It shows less transmittance change (ΔT) at 690nm owing to the thinner PB film

that in order to match the charge-density with a PolyRuFe film. Nevertheless, the ECD at 690 nm exhibits a short response time of less than 4 s. Furthermore, it is remarkable that the quite short response time of less than 0.5 s at 503 nm and 580 nm could be observed for both colored and bleached. It is attributed to the feature of the MEPE-based thin film. The photos of PolyRuFe/PB ECD at bleached (2.2 V) and colored (-1.3V) states are shown in **Figure 3(b)**.

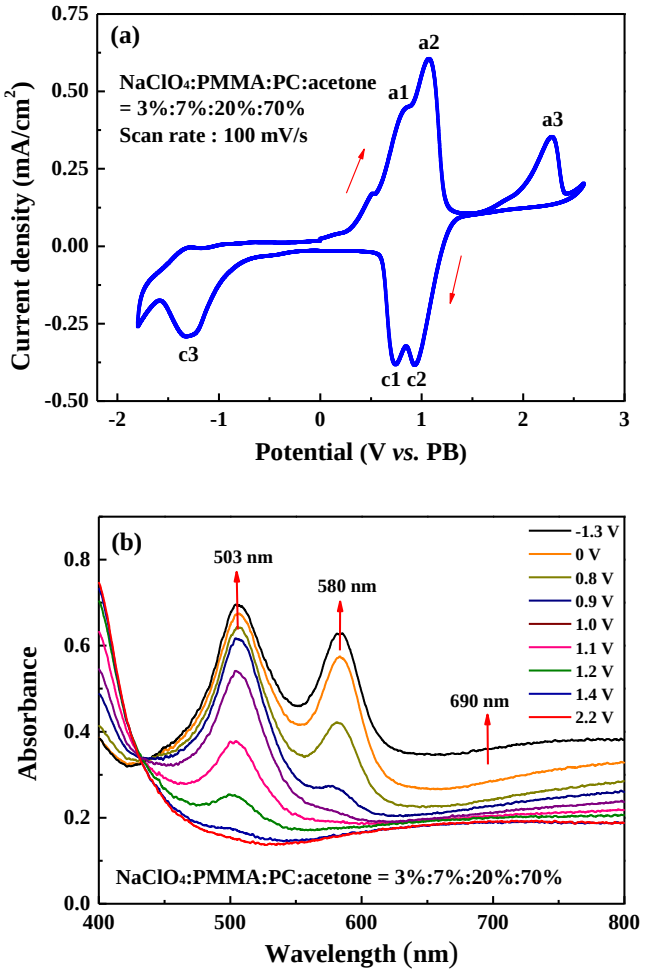

Figure 2. (a) CV of the PolyRuFe/PB ECD with the gel-typed electrolyte. (b) UV-vis absorbance spectra of the PolyRuFe/PB ECD obtained at different potential biases from -1.3 to 2.2 V.

Figure 3. (a) Dynamic transmittance response of the PolyRuFe/PB ECD at 503, 580 and 690 nm. (b) Images of the PolyRuFe/PB ECD at bleached (2.2 V) and colored (-1.3 V) states.

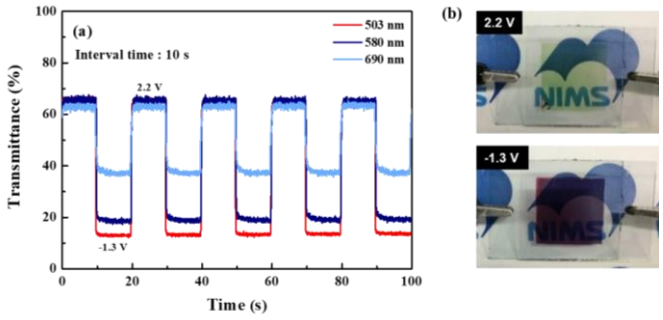

Table 1. Quantitative EC switching performance of the PolyRuFe/PB ECD at 503, 580 and 690 nm.

λ (nm)	T_b (%)	T_c (%)	ΔT (%)	t_b (s)	t_c (s)
503	66.3	13.6	52.7	0.3	0.2
580	66.2	19.3	46.9	0.5	0.3
690	64.5	36.5	28.0	0.9	3.6

To investigate the optical density change (ΔOD) and the required driving voltage for the PolyRuFe/PB ECD, the relationship between ΔOD at three different wavelengths and the charge density (Q_d) under various potential bias are presented in **Figure 4**. The measured charge densities were calculated by integration of the measured current densities against the fixing time (5 s). The coloration efficiency (η) is obtained by eqn. (5):

$$\eta = \Delta OD/Q_d \quad (5)$$

The coloration efficiencies of the PolyRuFe/PB ECD were calculated to be ca. 525.1, 61.4 and 57.7 cm^2/C at 503 nm; 114.3, 413.6 and 114.7 cm^2/C at 580 nm; 44.2 and 140.9 cm^2/C at 690 nm, corresponding to the portion of Ru(II), Fe(II), and Prussian blue, respectively. The value of coloration efficiency at 503 nm decreased dramatically while that at 503 nm increased at larger potential bias (0.9~2.2 V), which can be attributed to the prior reduction reaction of Ru(II) compared to Fe(II). In **Figure 2(a)**, the oxidation peak a1 of Fe(II) is on the left compared to the peak a2 of Ru(II), indicating the formal oxidation potential of Ru(II) is higher than Fe(II). In other words, Ru(II) is much easier reduced than Fe(II) so that Ru(II) was reduced first when applying a higher potential bias (0.9~2.2 V); while major part of Fe(II) was reduced when applying a smaller potential bias (0.6~0.9 V). Finally, the large absorbance change at 690 nm when applied potential bias from 0.6 to -1.3 V and coloration efficiency of PB was collected as 140.9 cm^2/C, which is the largest values, compared to 503 and 580 nm, upon these potential biases. These results explain the three-step values of the coloration efficiency for the proposed ECD. Furthermore, the quite large coloration efficiencies of 525.1 and 413.6 cm^2/C were obtained at 503 and 580 nm, respectively, suggesting that only a small charge density is needed to drive the two EC reactions (Eq. (1) and (2)). In addition, to scientifically evaluate the color change of ECD occurring on electrochemical switching, the ECD is subjected to colorimetric analysis by using CIE 1931 system of colorimetry, which is shown in **Figure S5**. When the device is at bleached state, the chromaticity coordinates (x=0.3391, y=0.3701). The chromaticity (x=0.3303, y=0.2428) could be observed at the colored state. The position at colored state in the chromaticity diagram moves toward purple area owing to the much stronger absorbance of PolyRuFe than that of PB.

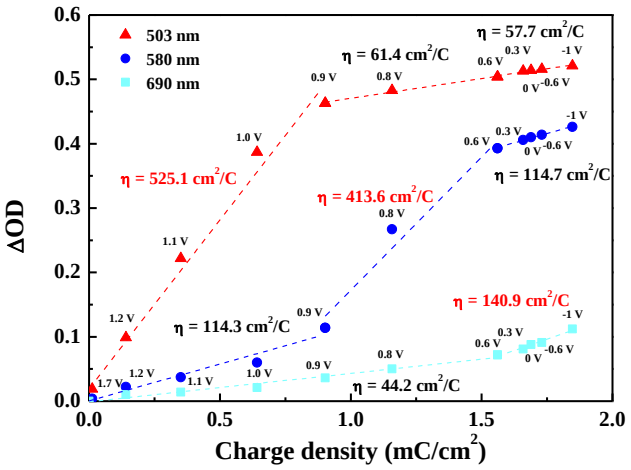

Figure 4. The relationship between the optical change (ΔOD) and the applied charge density with 5 s sampling time of the PolyRuFe/PB ECD at 503, 580 and 690 nm.

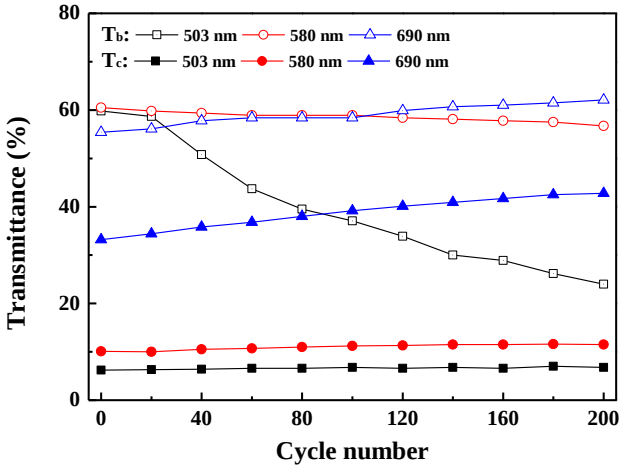

Figure 5. Transmittance data of the PolyRuFe/PB ECD as a function of cycle number. The ECD was switched between -1.3 and 2.2 V for 200 cycles.

A long-term cycling test for the PolyRuFe/PB ECD was performed and the results collected at 503, 580 and 690 nm are presented in **Figure 5**. No significant decay in ΔT could be observed at both 580 and 690 nm for 200 cycles, which are mainly contributed by PolyFe and PB respectively. By comparing the performances before and after 200 cycles (4000 s in total), its ΔT remains 89.7% and 89.6% of its original value (at 580 and 690 nm, respectively). However, the value of the ΔT at 503 nm decreased from the initial 53.6% to about 17.2% at the end of 200 cycles. PolyRu offers stable redox reactions in a three-electrode system, but may become unstable in the ECD owing to its higher redox potential. The reason to account for the difference in the long-term cycling stability is due to the poor memory effect of PolyRu, as compared to that of PolyFe. This leads to the ineffective preoxidation of PolyRuFe before preparing the ECD, which is generally considered to be a necessary step for assembling the ECD. To improve the poor memory effect of PolyRuFe, the multi-walled carbon nanotubes (MWCNTs) were introduced in the PolyRuFe thin film to form the PolyRuFe-MWCNT thin film. According to the literature,[52] oxidized MWCNTs would promote ClO_4^- adsorption due to the introduction of more oxygen-containing functional groups, which served as additional adsorption sites. The SEM images in **Figure S6** show (a) PolyRuFe and (b) PolyRuFe-MWCNT thin films prepared by spin-coating on ITO glasses. The surface of PolyRuFe is rather smooth and compact. In **Figure S6(b)**, the MWCNT is homogeneously dispersed into the PolyRuFe, forming the PolyRuFe-MWCNT. To compare the memory effect of the two thin films, the dynamic transmittance data were collected at 503 and 580 nm.

Both PolyRuFe and PolyRuFe-MWCNT thin films were reduced and oxidized under potential biases of 0 (colored state) and 1.3 V (bleached state), respectively, as shown in **Figure 6(a)**. After switching to the bleached state, the PolyRuFe film was left in an open-circuit condition to investigate its memory effect. The data for the transmittance retention are collected in **Table 2**. Under the open-circuit condition, PolyRu turns to the colored state rapidly in 50 s. On the other hand, PolyFe exhibits better memory effect which could maintain 40% of its saturated bleached state transmittance at 150 s. Due to the poor memory effect of PolyRu, it was found that PolyRu cannot maintain its bleached state for about 200 cycles under the long-term stability test. As shown in **Figure 6(b)** and **Table 2**, PolyRuFe-MWCNT exhibits better memory effect than that of the bare PolyRuFe at both wavelengths. PolyRuFe-MWCNT remained 75, 59, and 42% of their initial saturated bleached state transmittance at 503 nm after 50, 100 and 200 s, respectively. On the other hand, the transmittance retention of PolyRuFe-MWCNT at 580 nm increases to 94%. The memory effect of PolyRuFe-MWCNT was greatly increased, when compared with the bare PolyRuFe. Therefore, it is expected that by adding MWCNTs, the adsorption amount of ClO_4^- would increase, so as to enhance the memory effect of PolyRuFe.

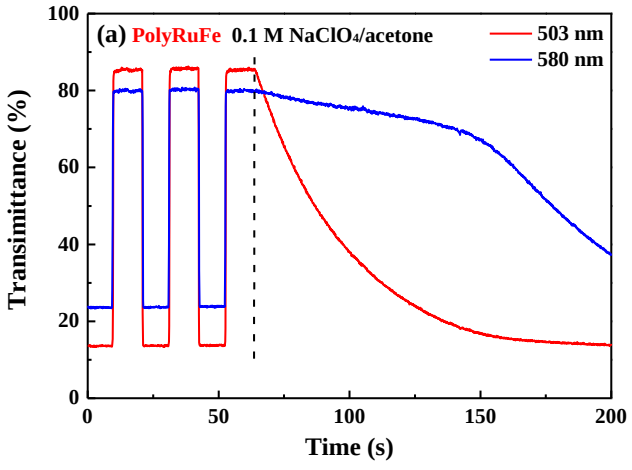

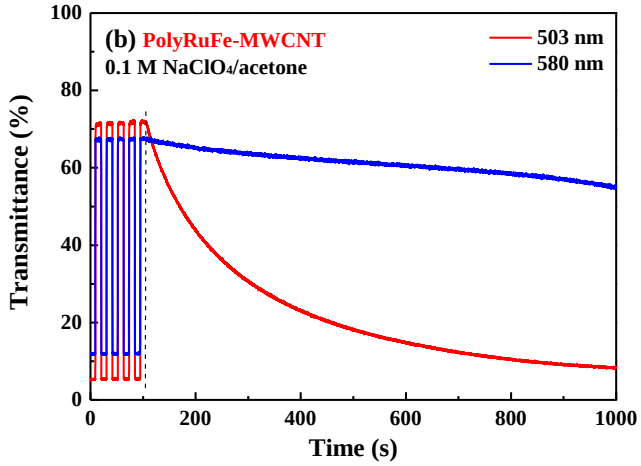

Figure 6. The variation of the transmittance after applying a bleached potential of 1.3 V and left in the OCV condition for (a) PolyRuFe and (b) PolyRuFe-MWCNT thin films at 503 and 580 nm.

Table 2. The memory effect, which can be expressed in terms of the percentage of the transmittance retention (R), for both PolyRuFe and PolyRuFe-MWCNT thin films.

Thin film	λ (nm)	T_b / R[a] (%) (initial)	T_b / R (%) (50 s)	T_b / R (%) (100 s)	T_b / R (%) (200 s)
PolyRuFe	503	85 / 100	29 / 34	15 / 18	-
	580	80 / 100	74 / 92	58 / 73	-
PolyRuFe-MWCNT	503	72 / 100	54 / 75	43 / 59	30 / 42
	580	67 / 100	66 / 98	65 / 96	64 / 94

[a] R is the percentage of the transmittance retention, which is defined as T_b to its initial value.

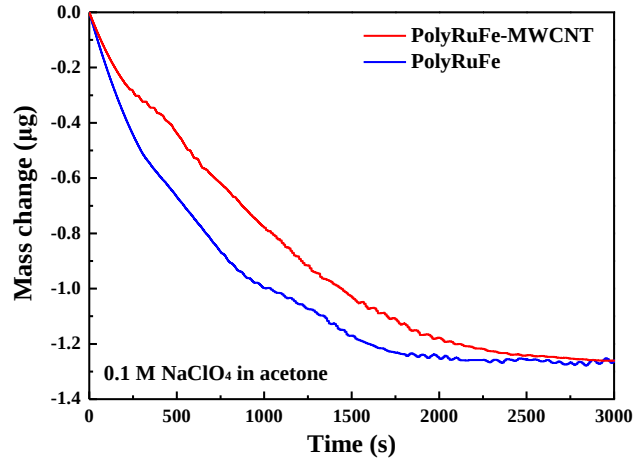

Figure 7. Mass changes of PolyRuFe-MWCNT and PolyRuFe thin films on the gold-disk electrode at the OCV.

Table 3. Quantitative mass changes of PolyRuFe and PolyRuFe-MWCNT thin films on the gold-disk electrode at OCV.

Thin film	ΔM[b] (μg) (500 s)	ΔM (μg) (1,000 s)	ΔM (μg) (1,500 s)	ΔM (μg) (2,000 s)	ΔM (μg) (3,000 s)
PolyRuFe	-0.67	-0.99	-1.17	-1.25	-1.26
PolyRuFe-MWCNT	-0.44	-0.78	-1.03	-1.18	-1.26

[b] ΔM is the mass change of either PolyRuFe-MWCNT or PolyRuFe thin film.

As mentioned earlier, perchlorate ion plays a crucial role in determining the memory effect of PolyRuFe. To understand the ionic transport phenomenon of ClO_4^- into PolyRuFe, the electrochemical quartz crystal microbalance (EQCM) analysis was utilized for studying PolyRuFe-MWCNT and PolyRuFe thin films. EQCM is used to quantify the mass changes in a gold-disk electrode by measuring the frequency change of the crystal. In order to calculate the accumulated mass (ΔM), a correlation equation is used, as shown in Eq. (6).

$$\Delta M = -[A \times N \times r_q / f_0^2] \times \Delta f \quad (6)$$

where ΔM is the change of mass (g), f_0 represents the resonant frequency of the initial mode of quartz crystal (8.88 MHz), A is the surface area of the gold-disk electrode (0.196 cm^2), N is the shear modulus of quartz (167 KHz cm), r_q is the density of the quartz crystal (2.684 g/cm^2), and Δf is the measured change of resonant frequency. **Figure S7(a)** and **(b)** show in situ mass change of PolyRuFe and PolyRuFe-MWCNT thin films during the potential cycling from 0 to 1.3 V in 0.1 M $NaClO_4$ at a scan rate of 20 mV/s, respectively. Both thin films show the reversible and stable mass change during the CV scan. When the cycling potential is switched from ca 0.7 to 1.2 V, increasing mass can be observed owing to the adsorption of ClO_4^-. On the other hand, when the potential is switched from ca 1.1 to 0.6 V, the decreasing mass was obtained due to the reduction of PoluRuFe, leading to the desorption of ClO_4^-. This indicates that the adsorption and desorption of ClO_4^- occurs accompanying the redox reaction of PolyRuFe, thus causing the mass changes of two thin films. The mass change was measured at the open-circuit voltage (OCV) condition, using a quartz crystal microbalance (QCM) so as to investigate the relationship between the memory effect and the adsorption of ClO_4-. The results are shown in **Figure 7**. The amounts of ClO_4- leaving from the PolyRuFe and PolyRuFe-MWCNT thin films were calculated and summarized in **Table 3**. The slower mass change of PolyRuFe-MWCNT can be observed at the OCV in 3,000 s, as compared to that of PolyRuFe, implying the effective adsorption of ClO_4^- by MWCNT. PolyRuFe-MWCNT thin film indeed exhibited better memory effect, which is attributed to the slower desorption of ClO_4^-. According to this result, effective capturing of the perchlorate ions is considered to be a key point to enhance the memory effect of PolyRu.

4. Conclusions

In this study, PolyRuFe which exhibited multi-color characteristic was successfully synthesized and the electrochromic properties were carefully investigated. The obtained PolyRuFe/PB ECD incorporating with the gel-typed electrolyte based on PMMA not only eliminates the leakage drawback of the liquid-type electrolyte, but also exhibits the panchromatic feature with high transmittance changes of 52.7, 46.9, and 28.0% at 503, 580 and 690 nm, respectively. Moreover, the short response time of less than 0.5 s could be observed at 503 and 580 nm for both colored and bleached, revealing one of the advantages of the MEPE-based films. In particular, the three-step values of the coloration efficiency could be observed in the proposed ECD. Ru(II) is much easier to be reduced than Fe(II) so that Ru(II) was reduced first when applying a higher range of potential bias (0.9 ~ 2.2 V); while the majority of Fe(II) was reduced when applying a lower range of potential bias (0.6 ~ 0.9 V); the large absorbance change at 690 nm was observed when applied further potential bias from 0.6 to -1.3 V. For the long-term stability, a significant decay could be observed at 503 nm, which is due to the poor memory effect of PolyRu, as compared to that of PolyFe. To improve the poor memory effect of PolyRu, MWCNTs were incorporated into PolyRuFe (PolyRuFe-MWCNT) to take the advantage of the ClO_4^- adsorption on the MWCNT. Compared to PolyRuFe, PolyRuFe-MWCNT exhibits better memory effect, which achieved 75, 59, and 42% of their initial saturated bleached state transmittance at 503 nm at durations of 50, 100 and 200 s, respectively. The mass change was monitored at the OCV condition, using a QCM to investigate the relationship between the memory effect and the adsorption of ClO_4^-, which verify the better memory effect of PolyRuFe-MWCNT.

Acknowledgment

This work was supported by JST CREST Grant Number JPMJCR1533, Japan. This work was also financially supported by the "Advanced Research Center for Green Materials Science and Technology" from The Featured Area Research Center Program within the framework of the Higher Education Sprout Project by the Ministry of Education (107L9006) and the Ministry of Science and Technology in Taiwan (MOST 104-2221-E-002-127-MY2, 105-2218-E-002-015, 107-3017-F-002-001).

References

1. I. Schwendeman, R. Hickman, G. Sönmez, P. Schottland, K. Zong, D. M. Welsh and J. R. Reynolds, *Chem. Mater.*, 2002, **14**, 3118-3122.
2. S.-Y. Kao, Y.-S. Lin, K. Chin, C.-W. Hu, M.-k. Leung and K.-C. Ho, *Sol. Energy Mater. Sol. Cells*, 2014, **125**, 261-267.
3. V. K. Thakur, G. Ding, J. Ma, P. S. Lee and X. Lu, *Adv. Mater.*, 2012, **24**, 4071-4096.
4. G. A. Niklasson and C. G. Granqvist, *J. Mater. Chem.*, 2007, **17**, 127-156.
5. C. G. Granqvist, *Thin Solid Films*, 2014, **564**, 1-38.
6. D. T. Gillaspie, R. C. Tenent and A. C. Dillon, *J. Mater. Chem.*, 2010, **20**, 9585-9592.
7. A. Ghicov and P. Schmuki, *Chem. Commun.*, 2009, **0**, 2791-2808.
8. K. Itaya, I. Uchida and V. D. Neff, *Acc. Chem. Res.*, 1986, **19**, 162-168.
9. M. Pyrasch, A. Toutianoush, W. Jin, J. Schnepf and B. Tieke, *Chem. Mater.*, 2003, **15**, 245-254.
10. K.-C. Chen, C.-Y. Hsu, C.-W. Hu and K.-C. Ho, *Sol. Energy Mater. Sol. Cells*, 2011, **95**, 2238-2245.
11. H.-C. Lu, S.-Y. Kao, H.-F. Yu, T.-H. Chang, C.-W. Kung and K.-C. Ho, *ACS Appl. Mater. Interfaces*, 2016, **8**, 30351-30361.
12. T.-H. Chang, C.-W. Hu, S.-Y. Kao, C.-W. Kung, H.-W. Chen and K.-C. Ho, *Sol. Energy Mater. Sol. Cells*, 2015, **143**, 606-612.
13. R. J. Mortimer and T. S. Varley, *Chem. Mater.*, 2011, **23**, 4077-4082.
14. Y. Alesanco, A. Viñuales, J. Palenzuela, I. Odriozola, G. Cabañero, J. Rodriguez and R. Tena-Zaera, *ACS Appl. Mater. Interfaces*, 2016, **8**, 14795-14801.
15. Y. Watanabe, K. Imaizumi, K. Nakamura and N. Kobayashi, *Sol. Energy Mater. Sol. Cells*, 2012, **99**, 88-94.
16. E. Poverenov, M. Li, A. Bitler and M. Bendikov, *Chem. Mater.*, 2010, **22**, 4019-4025.
17. M. T. Otley, F. A. Alamer, Y. Zhu, A. Singhaviranon, X. Zhang, M. Li, A. Kumar and G. A. Sotzing, *ACS Appl. Mater. Interfaces*, 2014, **6**, 1734-1739.
18. Y. Ding, M. A. Invernale, D. M. D. Mamangun, A. Kumar and G. A. Sotzing, *J. Mater. Chem.*, 2011, **21**, 11873-11878.
19. A. A. Argun and J. R. Reynolds, *J. Mater. Chem.*, 2005, **15**, 1793-1800.
20. M. Higuchi, *J. Mater. Chem. C*, 2014, **2**, 9331-9341.
21. J. B. Beck, J. M. Ineman and S. J. Rowan, *Macromolecules*, 2005, **38**, 5060-5068.
22. G. R. Whittell, M. D. Hager, U. S. Schubert and I. Manners, *Nat. Mater.*, 2011, **10**, 176.
23. P. K. Iyer, J. B. Beck, C. Weder and S. J. Rowan, *Chem. Commun.*, 2005, **0**, 319-321.
24. M. K. Bera, C. Chakraborty, U. Rana and M. Higuchi, *Macromolecular Rapid Communications*, 2018, **39**, 1800415.
25. S. Pai, M. Schott, L. Niklaus, U. Posset and D. G. Kurth, *J. Mater. Chem. C*, 2018, **6**, 3310-3321.
26. A. B. Atar, J. Y. Jeong, N. Kim and J. S. Park, *Macromolecular Research*, 2018, **26**, 814-818.
27. C.-J. Yao, Y.-W. Zhong and J. Yao, *Inorg. Chem.*, 2013, **52**, 10000-10008.
28. A. Winter and U. S. Schubert, *Chem Soc Rev.,* 2016, **45**, 5311-5357.
29. R. Dobrawa and F. Würthner, *J. Polym. Sci. A*, 2005, **43**, 4981-4995.
30. P. R. Andres and U. S. Schubert, *Adv. Mater.*, 2004, **16**, 1043-1068.
31. Y.-B. Dong, P. Wang, R.-Q. Huang and M. D. Smith, *Inorg. Chem.*, 2004, **43**, 4727-4739.
32. C. W. Hu, T. Sato, J. Zhang, S. Moriyama and M. Higuchi, *J. Mater. Chem. C*, 2013, **1**, 3408-3413.
33. F. S. Han, M. Higuchi, T. Ikeda, Y. Negishi, T. Tsukuda and D. G. Kurth, *J. Mater. Chem.*, 2008, **18**, 4555-4560.
34. M. Kanao and M. Higuchi, *J. Photopolym. Sci. Technol.*, 2015, **28**, 363-368.
35. F. S. Han, M. Higuchi and D. G. Kurth, *Org. Lett.*, 2007, **9**, 559-562.
36. M. Higuchi, *Yuki Gosei Kagaku Kyokaishi/Journal of Synthetic Organic Chemistry*, 2011, **69**, 229-235.
37. J. Zhang, C.-Y. Hsu and M. Higuchi, *J. Photopolym. Sci. Technol.*, 2014, **27**, 297-300.
38. P. M. Beaujuge, S. Ellinger and J. R. Reynolds, *Nat. Mater.*, 2008, **7**, 795.

39. C.-Y. Hsu, J. Zhang, T. Sato, S. Moriyama and M. Higuchi, *ACS Appl. Mater. Interfaces*, 2015, **7**, 18266-18272.
40. H. Shin, Y. Kim, T. Bhuvana, J. Lee, X. Yang, C. Park and E. Kim, *ACS Appl. Mater. Interfaces*, 2012, **4**, 185-191.
41. S. V. Vasilyeva, P. M. Beaujuge, S. Wang, J. E. Babiarz, V. W. Ballarotto and J. R. Reynolds, *ACS Appl. Mater. Interfaces*, 2011, **3**, 1022-1032.
42. J. T. Wu and G. S. Liou, *Chem. Commun.*, 2018, **54**, 2619-2622.
43. S.-Y. Kao, H.-C. Lu, C.-W. Kung, H.-W. Chen, T.-H. Chang and K.-C. Ho, *ACS Appl. Mater. Interfaces*, 2016, **8**, 4175-4184.
44. C.-W. Hu, T. Sato, J. Zhang, S. Moriyama and M. Higuchi, *ACS Appl. Mater. Interfaces*, 2014, **6**, 9118-9125.
45. M. Chiper, M. A. R. Meier, D. Wouters, S. Hoeppener, C.-A. Fustin, J.-F. Gohy and U. S. Schubert, *Macromolecules*, 2008, **41**, 2771-2777.
46. J. Yang, J. K. Clegg, Q. Jiang, X. Lui, H. Yan, W. Zhong and J. E. Beves, *Dalton Transactions*, 2013, **42**, 15625-15636.
47. J. W. McCargar and V. D. Neff, *J. Phys. Chem.*, 1988, **92**, 3598-3604.
48. R. J. Mortimer and J. R. Reynolds, *J. Mater. Chem.*, 2005, **15**, 2226-2233.
49. M.-S. Fan, S.-Y. Kao, T.-H. Chang, R. Vittal and K.-C. Ho, *Sol. Energy Mater. Sol. Cells*, 2016, **145**, 35-41.
50. K.-M. Lee, H. Tanaka, A. Takahashi, K. H. Kim, M. Kawamura, Y. Abe and T. Kawamoto, *Electrochimica Acta*, 2015, **163**, 288-295.
51. L. Su, J. Fang, Z. Xiao and Z. Lu, *Thin Solid Films*, 1997, **306**, 133-136.
52. Q. Fang and B. Chen, *Carbon*, 2012, **50**, 2209-2219.
53. A. Gotoh, H. Uchida, M. Ishizaki, T. Satoh, S. Kaga, S. Okamoto, M. Ohta, M. Sakamoto, T. Kawamoto, H. Tanaka, *Nanotechnology*, 2007, **18**, 345609.

Graphical abstract

A panchromatic electrochromic device composed of Ru(II)/Fe(II)-based heterometallo-supramolecular polymer

Li-Yin Hsiao,[a, d] Ting-Hsiang Chang,[a] Hsin-Che Lu,[a] Yen-Chun Wang,[a] Yen-An Lu,[a]

Kuo-Chuan Ho,[a, b, c]* and Masayoshi Higuchi[d]*

[a] Department of Chemical Engineering, National Taiwan University, No. 1, Sec. 4, Roosevelt Road, Taipei 10617, Taiwan

[b] Institute of Polymer Science and Engineering, National Taiwan University, Taipei 10617, Taiwan

[c] Advanced Research Center for Green Materials Science and Technology, National Taiwan University, Taipei 10617, Taiwan

[d] Electronic Functional Macromolecules Group, Research Center for Functional Materials, National Institute for Materials Science (NIMS), Tsukuba 305-0044, Japan

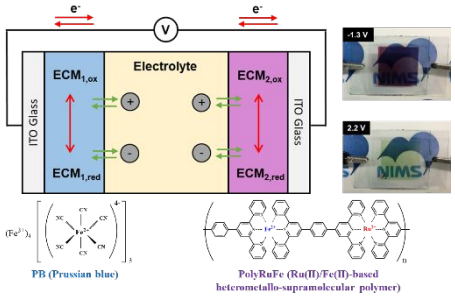

A panchromatic electrochromic device composed of PolyRuFe and Prussian blue is proposed in this study and the memory effect of PolyRuFe is improved by incorporating with multi-walled carbon nanotubes.